

RESEARCH ARTICLE

A simple method for rapid removal of the memory effect in cavity ring-down spectroscopy water isotope measurements

Jonathan Keinan^{1,2}  | Yonaton Goldsmith¹ ¹Institute of Earth Sciences, The Hebrew University of Jerusalem, Jerusalem, Israel²Geological Survey of Israel, Jerusalem, Israel**Correspondence**

J. Keinan, Institute of Earth Sciences, The Hebrew University of Jerusalem, Jerusalem 9190401, Israel.

Email: jonathan.keinan@mail.huji.ac.il**Funding information**

Israel Science Foundation, Grant/Award Number: 2229/21; Climate Crisis Scholarship of the Jewish National Fund

Rationale: The accuracy determined in the routine analysis of water isotopes ($\delta^{17}\text{O}$, $\delta^{18}\text{O}$, $\delta^2\text{H}$) using cavity ring-down spectroscopy is greatly affected by the memory effect (ME), a sample-to-sample carryover that biases measurements. This study aims to develop a simple method that rapidly removes the ME.

Methods: We developed a method, designed for the Picarro L2140-i, that removes the ME by injecting small amounts of water with an extreme isotopic value (“kick”) in the opposite direction of the ME. We conducted 11 experiments to identify the optimal kick for pairs of isotopically enriched and depleted samples. Once quantified, the optimal kick was used to create an ME-free, unbiased calibration curve, which was verified using international and internal lab standards.

Results: Our kick method removes the ME very efficiently in half the time it takes for experiments without a kick. The optimal number of kick injections required to minimize stabilization time between standards of different compositions is three injections of $\delta^2\text{H} \approx -1000\%$ water per a 100‰ difference between standards. Three runs of routine measurements using the kick method resulted in uncertainties of 0.03‰, 0.2‰, and 5 permeg for $\delta^{18}\text{O}$, $\delta^2\text{H}$, and ^{17}O -excess, respectively.

Conclusions: This study demonstrates a new method for rapidly removing the ME. Our kick protocol is a readily available, cheap, and efficient approach to reduce instrumental bias and improve measurement accuracy.

1 | INTRODUCTION

The accuracy of stable isotopic measurements lies at the foundation of isotope geochemistry. In recent decades, the use of laser absorption spectrometric instruments for isotopic measurements of water has dramatically increased.^{1–5} These instruments are small, require no sample preparation and a significantly smaller sample size, and can simultaneously measure triple oxygen and hydrogen isotopes ($\delta^{18}\text{O}$, $\delta^{17}\text{O}$, and $\delta^2\text{H}$), while achieving similar or arguably better precision than conventional isotope ratio mass spectrometers (IRMS).^{4,6–8} Many studies have noted that, despite their numerous advantages and growing popularity, laser-based measurements of

water isotopes are affected by a sample-to-sample carryover, known as the memory effect (ME), which reduces their accuracy and precision.^{9–11} Observations show that when running two samples consecutively on laser-based instruments, the measurements of the second sample are shifted in the direction of the first and, therefore, contain its “memory.”^{2,9,12–15} The ME is particularly apparent between samples that have different isotope ratios and is most apparent in hydrogen isotopes. The ME is a substantial pitfall that limits the accuracy and precision when calibrating lab standards and during routine measurements.^{2,8,10} Yet, over half of the laboratories that perform laser absorption spectrometry do not correct for the ME,³ and an astonishing 70% of them are unable to replicate a blind

This is an open access article under the terms of the [Creative Commons Attribution-NonCommercial-NoDerivs](https://creativecommons.org/licenses/by-nc-nd/4.0/) License, which permits use and distribution in any medium, provided the original work is properly cited, the use is non-commercial and no modifications or adaptations are made.

© 2023 The Authors. *Rapid Communications in Mass Spectrometry* published by John Wiley & Sons Ltd.

duplicate measurement to their claimed precision.⁴ Therefore, to utilize the full potential of these instruments, minimizing the ME is a cardinal goal that cannot be overlooked.

The physical reason for the ME is that water molecules adsorb onto surfaces due to hydrogen bonding, which is a well-known phenomenon in vacuum technology.^{16,17} Replacing ordinary hydrogen with deuterium increases binding energy and, consequently, also the residence time of deuterated water molecules on the internal surfaces of vacuum systems. Laser-based systems commonly include a vaporizing chamber and an optical cavity operating in vacuum conditions (for full details of instrument components, see Berman et al⁷ or Steig et al⁶). Liquid water samples are injected into a vaporizer using an autosampler, and from there, the water vapor is transported into an optical cavity for measurement. As the previous water sample is adsorbed onto the vaporizer and optical cavity and is not fully removed, the water from the next injected sample gets mixed in with the previously adsorbed water, causing the ME. This adsorption is strongest for $^1\text{H}^2\text{H}^{16}\text{O}$ isotopologue relative to $^1\text{H}^1\text{H}^{16}\text{O}$, $^1\text{H}^1\text{H}^{18}\text{O}$, or $^1\text{H}^1\text{H}^{17}\text{O}$, which leads to a stronger ME for $\delta^2\text{H}$ measurements. In addition to the tendency of water vapor to adhere to the internal surfaces of the instrument,⁹ the ME could also occur because of a carryover from a previous sample by the sampling syringe.¹⁸

The ME is expected to be the main factor reducing the precision and accuracy compared with the basic specifications of the instrument;⁸ therefore, an in-depth exploration of its impact and the appropriate correction strategies is required. In the following list, we describe the main approaches that have been proposed for ME corrections and address the potential drawbacks of each suggestion:

1. Discarding of injections—a common and simple approach is to discard initial injections^{7,10,13,15,19} or give them reduced weights.²⁰ This is also the manufacturer's recommendation. For the Picarro wavelength-scanned cavity ring-down spectroscopy (WS-CRDS) instrument, the manufacturer specifies the magnitude of the ME as a percentage of the final value, being better than 98% (for $\delta^2\text{H}$ values) and 99% (for $\delta^{17}\text{O}$ and $\delta^{18}\text{O}$ values) after the fourth injection, and recommends simply discarding the first few injections in data processing.
2. Ordering—minimizing the ME by ordering samples according to their isotopic composition (e.g., Schauer et al⁸). Usually, the expected isotopic compositions are roughly known. The problem may occur when calibrating internal lab standards that require a large isotopic spread or in cases where the samples vary greatly in their isotopic composition.
3. Conditioning—injecting a sample of similar composition before the sample of interest (e.g., van Geldern and Barth¹⁰). Conditioning is relevant only if very small quantities of the sample are available. In most cases, users can simply administer a few more injections into a measurement run or separate the sample into two vials, considering the first one as a “conditioner” vial (e.g., Schauer et al⁸). This is handy because numerous injections from the same

vial may result in an evaporative fractionation. According to Schauer et al,⁸ the most effective tools against the ME are the conditioning vials and the selective sequence of waters; however, they are cautious and state that their approach does not fully remove the ME.

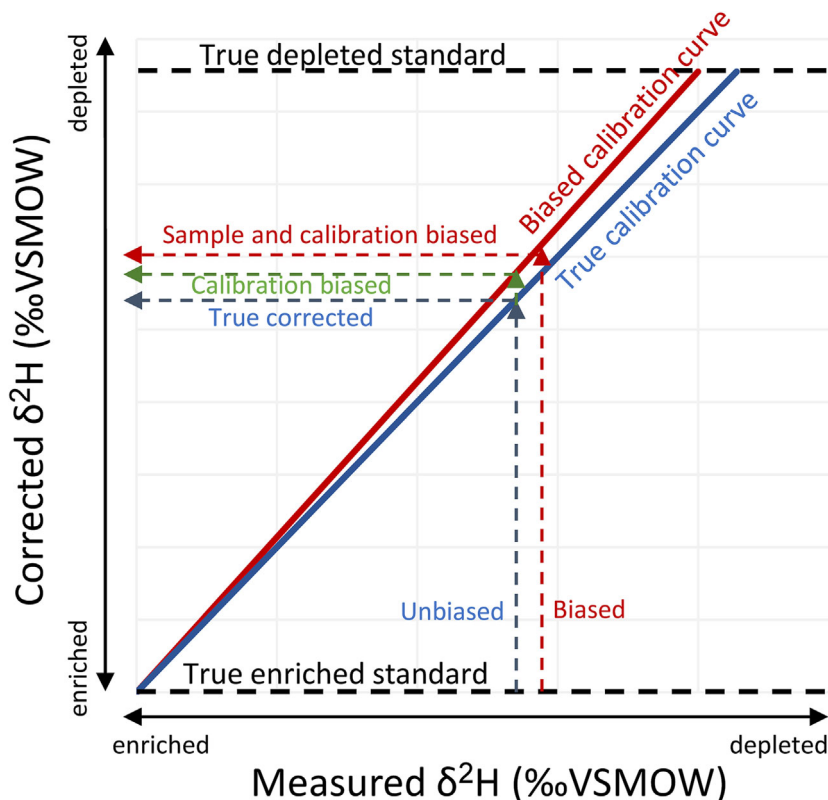
4. Estimation—the ME is characterized by measuring known samples and developing a memory-correction equation.^{8,15,21–24} For example, Guidotti et al²¹ proposed the three-pool model, in which each measured sample is a mixture of three pools of water that have different sizes and exchange rates. They showed that the method can correct huge memory signals, without the need for “true” values. Although this method is useful for isotopically modified samples (e.g., which vary by over 25 000‰ as used in biological and medicinal-related research), for natural water compositions, it has been shown to cause a major overcorrection.¹³

In addition, estimation has been shown to be problematic, and a comparison of different correction methods gave varying results, depending on the difference between the isotopic composition of the samples.¹³ Furthermore, estimation techniques rely on the assumption that the ME does not decrease further with the increase in the number of injections, and the measurement result for the last injection is memory free.¹⁵ According to Vallet-Coulomb et al,¹³ 45 injections are enough to erase all ME for a sample-to-sample difference of $\delta^2\text{H} = \sim 204\text{‰}$.

5. Moisturizing the carrier gas—de Graaf et al¹² constructed a setup in which water vapor of known isotopic composition is added to the carrier gas and the injected sample is analyzed based on its difference from the background gas. This method requires a short measurement time and appears to be the fastest documented setup to eliminate the ME. This method achieves excellent precision for $\delta^2\text{H}$ and $\delta^{18}\text{O}$. However, a major drawback is that internal precision (1σ) on a single injection for $\delta^{17}\text{O}$ is between 0.11‰ and 0.15‰ and for ^{17}O -excess, between 50 and 60 permeg, which is an order of magnitude larger than that currently accepted. Therefore, although this is a fast and remarkable setup for $\delta^2\text{H}$ and $\delta^{18}\text{O}$ measurements, it is unsatisfactory for most scientific applications requiring ^{17}O -excess and requires a specifically designed inlet system.

These methods are most useful when running samples with small isotopic variations, which is the most common application for such instruments. However, these methods are not sufficient when constructing the Vienna Standard Mean Ocean Water (VSMOW) – Standard Light Antarctic Precipitation (SLAP) scale as recommended by Schoenemann et al.²⁵ This is due to the large differences between VSMOW2 (0‰ and 0‰, for $\delta^2\text{H}$ and $\delta^{18}\text{O}$, respectively) and SLAP2 (–427.5‰ and –55.5‰, for $\delta^2\text{H}$ and $\delta^{18}\text{O}$, respectively), which leads to a significant ME that cannot be overcome by these methods (Figure 1). This carryover biases the fundamental calibration curve, which is one of the most important and sensitive steps in a laboratory setup, and is thus a fundamental

FIGURE 1 Illustration of how an ME-biased VSMOW–SLAP calibration curve can affect all measured samples. The horizontal axis is measured values. The vertical axis is corrected (true) values. The calibration of water isotopes is based on the VSMOW–SLAP calibration curve,²⁵ two primary standards that have very different isotopic values. When running SLAP2 after VSMOW2, if the ME is not sufficiently eliminated, the measured SLAP2 value would be heavier than true values, and the corresponding calibration curve (red filled line) would be shifted with respect to an unbiased curve (blue line). An unknown sample (horizontal dashed blue line) corrected using the biased calibration curve would be offset from the true value (horizontal dashed green line). If this sample also experienced an ME during measurement, a second bias would be introduced, shifting the measurement toward more negative values (horizontal dashed red line). The bias would be greater for more depleted samples (as they are closer to the ME-affected SLAP2). The biases shown are exaggerated for illustration purposes (in reality, this bias is $\sim 1\%$ for $\delta^2\text{H}$). ME, memory effect. [Color figure can be viewed at wileyonlinelibrary.com]



problem. To illustrate the magnitude of this problem, we present a theoretical but common example of this calibration bias (Figure 1). During the VSMOW–SLAP instrumental calibration in a Picarro WS-CRDS, the manufacturer-certified ME carryover of 2% for $\delta^2\text{H}$ and 1% $\delta^{18}\text{O}$ after the fourth injection would result in a biased $\delta^2\text{H}$ calibration curve of $\sim 8.5\%$ and $\sim 0.55\%$ for $\delta^2\text{H}$ and $\delta^{18}\text{O}$, respectively (Figure 1). Applying this calibration curve to a hypothetical sample with a composition of $\delta^2\text{H} \sim -150\%$ and $\delta^{18}\text{O} \sim -20\%$ would result in an accuracy bias of 2.5% and 0.2% for $\delta^2\text{H}$ and $\delta^{18}\text{O}$ values, respectively. This accuracy bias is much larger than the certified instrumental precision, and, more importantly, biases every sample run on the instrument.

A second place where the ME has a substantial effect on measurement accuracy occurs while running in-house internal lab standards during routine analysis. Proper normalization requires at least two standards, ideally bracketing the expected range of sample values. Pierchala et al.¹⁵ conducted an in-depth analysis of the combined uncertainty of a single measurement result and showed that the assigned uncertainty of the calibration standards is an important component of the total uncertainty, especially in the case of $\delta^2\text{H}$. Neglecting it can lead to serious underestimation of measurement uncertainty. When the difference between the bracketing standards is small, the measurement uncertainty rises.^{15,26} However, when the difference between the bracketing standards is large, the ME is more pronounced, biasing the accuracy.

The combination of these two biases (the biases of the primary calibration curve and the routinely used lab standards calibration curve), which work in the same direction, can cause bias for every measurement corrected based on these two sets of calibration curves (Figure 1). As the calibration curve is a self-consistent framework that does not have the ability to assess its own accuracy, it is impossible to detect these two biases and thus the trueness of the isotopic value.

In this study, we present a new and simple method that quickens the ME removal when constructing the VSMOW–SLAP calibration curve and can thus improve the accuracy of internal lab standards and routine measurements. The ME is caused by incomplete removal of the previous sample that creates mixing between consecutive samples. A possible way to reduce the lingering of the ME is by flushing the system with water that counteracts the ME in the opposite direction (a “kick”), aiming for a mixing that is roughly identical to that of the next sample to be analyzed. In other words, we hypothesized that the layover of ME-enriched samples can be offset by several injections of extremely depleted water before the injection of the next sample; this minimizes the time required for ME removal and can enhance the instrument's accuracy. For example, when measuring the VSMOW–SLAP calibration curve, after running VSMOW2 ($\delta^2\text{H} = 0\%$), the system is flushed with extremely depleted water ($\delta^2\text{H}$ of $\sim -1000\%$) before measuring SLAP2 ($\delta^2\text{H} = -427.5\%$). In this paper, we characterize the ME and ME-free runs, construct 11 experiments to test the magnitude of the

isotopically light kick in various conditions, and validate the method for both lab standard calibration (by measuring certified water standards) and routine measurements (using in-house quality control standards treated as unknowns).

2 | METHODS

2.1 | Instrumental setup

We used a Picarro L2140-i isotopic analyzer (Picarro, Santa Clara, CA, USA) to simultaneously measure the $\delta^{17}\text{O}$, $\delta^{18}\text{O}$, and $\delta^2\text{H}$ values and derive the values of ^{17}O -excess (described in detail by Steig et al.,⁶ section 2.3.1). Liquid water samples were stored in 2 ml glass vials capped with blue polypropylene caps with red polytetrafluoroethylene/white silicone septum and injected with a liquid autosampler (Picarro A0325) into a vaporizer module (Picarro A0211), using pure nitrogen (99.999%) as the carrier gas. A 10 μl syringe was used to collect and inject discrete liquid samples, targeting a water vapor concentration of 20 000 ppm, which in our system requires 3.2 μl of the sample. The manufacturer-supplied coordinator software was run on the factory default “ ^{17}O High Precision” mode, giving an output of relatively user-friendly comma-separated values files, which were postprocessed using a Python script (Supporting Information). To minimize syringe actuation and possible fractionation due to evaporation or mixing of a penetrated cap, the syringe was not rinsed between vials. Instead, the water was injected into the vaporizer to flush out the ME of the previous sample. Each injection is an average of ~ 220 ring-down cycles and takes approximately 9 min. The built-in coordinator software integrates the ring-down cycles into a single value and provides statistical information useful for identifying problematic measurements and/or the lingering of the ME (described below). To reduce uncertainty, multiple injections of each sample are measured, and the average and SD of these injections are reported. Instrumental noise can be identified as a large SD or slope of a single measurement (intra-injection noise of the ring-down cycles) and/or as a large SD and consistent trend between measured injections of the same sample (inter-injection slope).

2.2 | Methodology and developing protocol

2.2.1 | Quantifying measurement precision of ME-free samples

The first stage of assessing the ME is defining objective criteria for stable ME-free measurements. To assess ME-free measurements, a standard precision and drift test was run for 6 days (900 injections of water from a 60 ml container in the wash station). Using these measurements, we first assessed the intra-injection parameters of an individual injection: SD and slope of the ring-down cycles. Then, we

assessed the inter-injection SD and slope using batches of 15 consecutive injections as well as the long-term SD values and instrumental drift. The number of injections selected for evaluating the inter-injection slope ($n = 15$) is based on current literature regarding the adequate number of injections for achieving high precision results for in-house lab standard calibrations,^{13–15} also used by the top-performing laboratory in the 2020 International Atomic Energy Agency (IAEA) Water Isotope Inter-Comparison test.⁴

2.2.2 | Characterizing of the ME

The second stage of experiments is intended to characterize the ME. The ME is the unidirectional evolution of a series of injections; therefore, the existence of an inter-injection slope indicates the presence of the ME. By monitoring the magnitude of the inter-injection slope, we can assess the ME's magnitude and identify when it disappears. To characterize the inter-injection slope of the ME, we measured an enriched water sample (200 injections of $\sim 0\%$, similar to VSMOW), followed by a depleted water sample (200 injections of $\sim -450\%$, similar to SLAP2), after which the instrument was flushed with pure N_2 for 30 h and then injected again with an enriched water sample (200 injections of $\sim 0\%$). Throughout the experiment, we monitored and characterized the magnitude of the inter-injection slope.

2.2.3 | Characterization of the kick method

In this part of the paper, we introduce and examine the effects of our proposed kick method. Our method entails injecting extremely depleted water into the system to flush out the effect of relatively enriched water. The success of using a humidified carrier gas to eliminate the ME¹² proves that the only way to physically remove water vapor adsorbed to the surfaces of the instrument is by replacing it with the vapor of a different composition. Our method uses this logic but is based on a much simpler setup; it requires only a vial with extremely depleted water that is used to “mix away” the ME. To test the kick method, we constructed 11 experiments; in each, we ran a sequence of an enriched sample, followed by a designated number of kick injections and then a depleted sample. In each experiment, we varied the number of kick injections and/or the isotopic difference between enriched and depleted samples. The goal of these experiments was to assess whether the kick method can reduce the time (i.e., number of injections) required for the removal of the ME and quantify the optimal magnitude of the kick for each set of enriched and depleted samples. In other words, the goal is determine whether the number of kick injections required to remove the ME is a function of the difference between the two samples. The run architecture for this characterization test was (1) 200 injections of an enriched sample, (2) varying numbers of kick injections of an extremely depleted water (commercially available deuterium depleted water with $\delta^2\text{H}$ values of $\sim -1000\%$), and (3) 200 injections

of a depleted sample. We expect that there should be an ideal number of kick injections that removes the ME most efficiently. The magnitude of the optimal kick is expected to be proportionate to the difference between the enriched and depleted samples. An insufficient kick (i.e., not enough injections) will cause the ME of the enriched samples to prevail. An excessive kick (i.e., too many injections) will cause the depleted sample to experience the ME of the kick (i.e., the ME will become too negative).

2.2.4 | Validation 1: Testing the kick method for known international standards

To validate whether the kick method works, we constructed a VSMOW–SLAP calibration curve using the kick method to remove the ME VSMOW2 creates on SLAP2. We tested the accuracy of this calibration curve against a set of secondary international standards (from the United States Geological Survey [USGS] and IAEA) and internal and external lab standards, run after the initial calibration curve. The secondary standards were ordered from the most isotopically depleted to the most enriched (Table 1). At the end of the run, VSMOW2 and SLAP2 were measured again in the same order (conditioning vials and kick). To prevent possible enrichment of the isotopic composition by evaporation, each vial was preceded by a conditioning vial of the same or similar composition.¹³ The vaporizer septum was replaced in the middle of the run before a conditioning vial.

To normalize samples' $\delta^{17}\text{O}$, $\delta^{18}\text{O}$, and $\delta^2\text{H}$ to the VSMOW–SLAP scale,²⁵ we constructed initial and final VSMOW2–SLAP2 calibration curves and assumed that the instrumental drift was linear between them (which was confirmed by our 6-day precision

and drift test). For each calibration curve, a measured versus expected linear plot was created using the York method.²⁷ This method creates a best-fit calibration line that assumes uncertainty in both axes (i.e., the uncertainty of the primary standards and the measurement uncertainty) and results in uncertainties for both the slope and intercept of the calibration curve, which is crucial for proper error propagation.^{3,4,14,15} The uncertainties of the standards are as published by IAEA and USGS,^{28–36} and the uncertainty of the measured values are the standard error (SD divided by the square root of the number of injections used). To correct for possible drift throughout the run, samples were proportionately corrected to the relative measuring time from the initial and final calibration curves using inverse distance weights (e.g., if 10 samples were run, the first sample would be weighed 90% to the initial calibration curve and 10% to the final calibration curve). The entire architecture, which spans over ~ 3 days, was repeated four times (Table 1). Detailed information, error propagation calculations, and Python script are given in the [Supporting Information](#).

2.2.5 | Validation 2: Testing the kick method during routine measurements

To test the implementation of our kick method during routine measurements, we conducted three experiments that mimic a routine measurement sequence using the kick method and evaluated the accuracy of the known quality assurance standards interspersed within unknown samples. The architecture is identical to the standards calibration sequence (Table 1), beginning with a conditioning vial of an enriched calibration internal lab standard,

TABLE 1 Run architecture used to validate the kick method and calibrate in-house standards.

Vial position	Identifier	Purpose	True $\delta^2\text{H}$ value (‰ _{VSMOW})	Number of injections
1	VSMOW2_cond	Conditioner	0	15
2	VSMOW2	High δ value primary standard for calibration	0	15
3	Litewater	Kick	~ -1000	13
4	SLAP2_cond	Conditioner	-427.5	40
5	SLAP2	Low δ value primary standard for calibration	-427.5	20
6–27	Standards and samples arranged from depleted to enriched consisting of 13 conditioning and 13 sample injections	Certified standards for method verification and internal lab standards for calibration	Variable	13
1	VSMOW2_cond	Conditioner	0	15
2	VSMOW2	High δ value primary standard for calibration	0	15
3	Litewater	Kick	~ -1000	13
4	SLAP2_cond	Conditioner	-427.5	40
5	SLAP2	Low δ value primary standard for calibration	-427.5	20

Note: To prevent possible enrichment of the isotopic composition by evaporation, each vial was preconditioned with a vial of the same or similar composition. The entire architecture, which spans over ~ 4 days, was repeated four times.

followed by 15 injections of the standard, the optimal number of kick injections of extremely depleted water, and then a sufficient number of conditioning low standard injections followed by injecting the low standard. After running the standards, a sequence of unknown samples was run, and quality assurance standards were interspersed within these unknown samples. At the end of the run, the high and low standards are measured again in the same order, including kick and conditioning vials.

3 | RESULTS AND DISCUSSION

3.1 | Criteria for ME-free measurements of single and multiple injections

In this section, we present and discuss objective criteria for defining ME-free measurements. We focus on $\delta^2\text{H}$ values, which have been shown to be most affected by instrumental drift and the ME

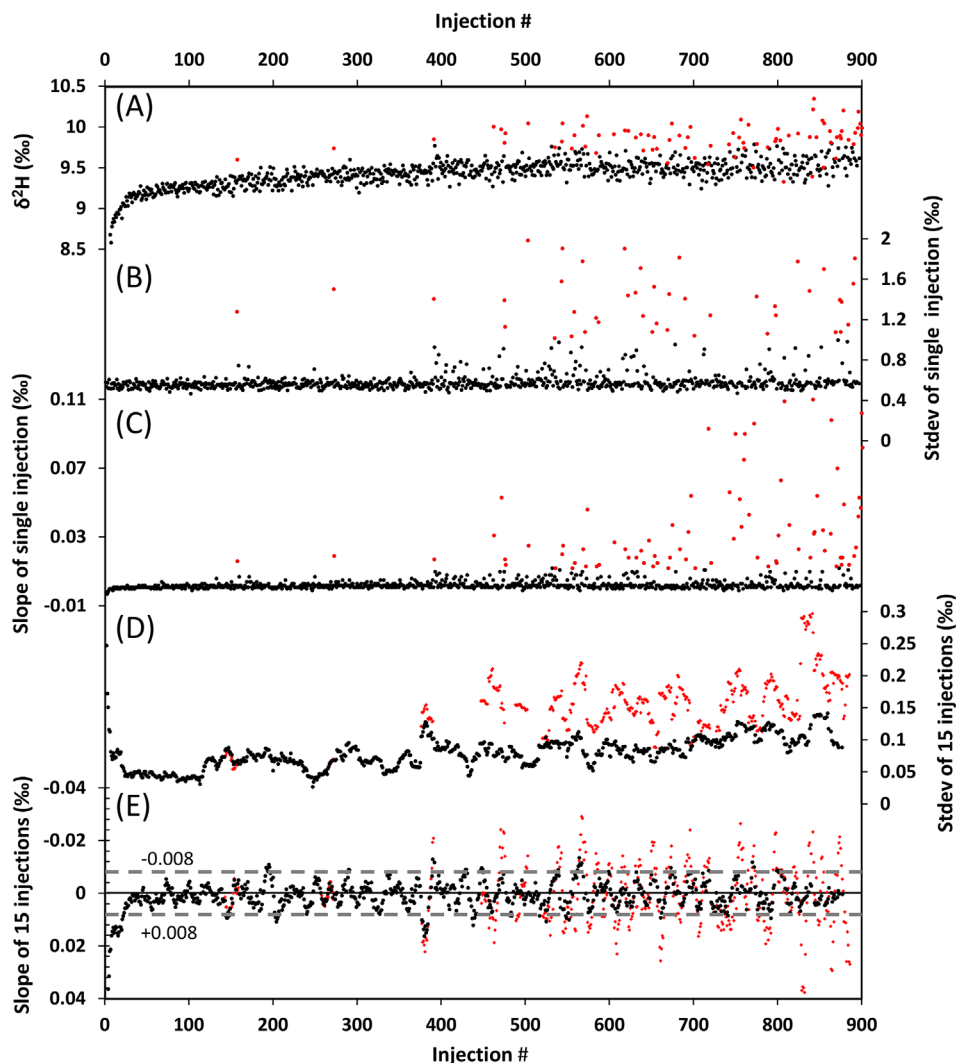


FIGURE 2 Characterizing ME-free measurements. Parameters for quality assurance were assessed using a 6-day standard precision and drift test. Panels A–C show unmodified data acquired by the coordinator software running on ^{17}O high precision mode. Each injection and analysis duration is 9 minutes. Acquisition rate is ~ 1 Hz, and therefore each injection is composed of the average of 1 Hz data points across the water pulse (~ 220 individual ring-down cycles). A, $\delta^2\text{H}$ values of single injections (black) and $\delta^2\text{H}$ values of injections discarded by single injection criteria from panels B and C (red). B, SD of the measured $\delta^2\text{H}$ of each single injection. Measurements that have an intra-injection SD < 1 (black) and SD > 1 (red). C, Intra-injection slope of the measured $\delta^2\text{H}$ of each single injection. Samples that have an absolute value of $|\text{Slope}| \leq 0.005$ (black) and $|\text{Slope}| > 0.005$ (red). D, SD of 15 consecutive injections. Samples that pass the criteria from panels B and C (black) and those that do not (red). E, Slope15 index—the slope of the proceeding 15 injections acquired by linear regression. Samples that pass the criteria from panels B and C (black) and those that do not (red). Stabilized ME-free measurements exhibit a Slope15 of less than ± 0.008 and oscillate around 0. This range is marked by the horizontal dashed lines. Based on these results, we define samples that exhibit a Slope15 > 0.008 as affected by the ME. ME, memory effect. [Color figure can be viewed at wileyonlinelibrary.com]

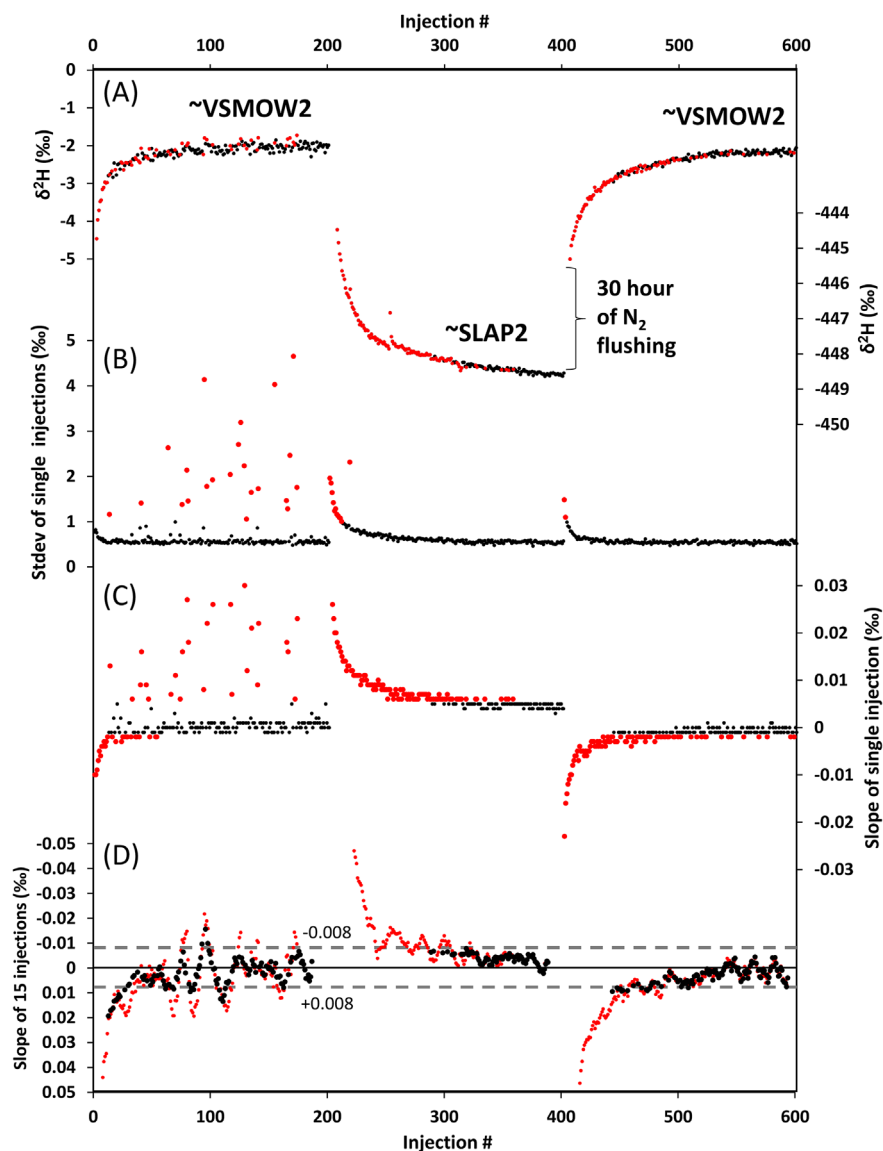
(e.g., Vallet-Coulomb et al¹³). We first examined the characteristics of single injections during a multiday precision and drift test, which defines typical instrumental noise and long-term instrumental drift (Figure 2). Each injection averages ~ 220 ring-down cycles in the instrument's cavity. The SD and slope of these ring-down cycles provide a means for characterizing the behavior of each single injection. Over 90% of the single injections exhibit an intra-injection SD of less than 1‰ and an intra-injection slope of $<0.005\%$ throughout the ring-down cycles (Figures 2B and 2C). We use these criteria to define a threshold above which single injections are discarded. Most of these failed injections occur after injection ~ 400 and can be easily accounted for by changing the injection port septum—every 200–300 injections, as recommended by the manufacturer.

The inter-injection SD ($\pm 1\sigma$) of $\delta^2\text{H}$ for 15 consecutive injections is 0.11 (± 0.06)‰ (Figure 2D and Table S1 [supporting information]),

and the slope of 15 consecutive injections is 0.0008 (± 0.008) (Figure 2E and Table S1 [supporting information]). Discarding injections that failed the intra-injection criteria results in improved inter-injection SD and slope of 0.08 (± 0.02)‰ and 0.0006 (± 0.005)‰, respectively. These results show that there is no inter-injection slope throughout this experiment and, thus, no ME. We use these results to define an ME-free measurement: an injection is ME-free if the next 15 injections do not exhibit an inter-injection slope of $|\text{Slope}_{15}| \leq 0.008\%$ for $\delta^2\text{H}$. Evaluating Slope_{15} for $\delta^{18}\text{O}$ and ^{17}O -excess results in much lower values (0.0001 [± 0.0034]‰ and 4×10^{-6} [± 0.0009]‰), respectively; Table S1 [supporting information]), and, therefore, we use the more sensitive Slope_{15} of $\delta^2\text{H}$ to evaluate the existence of the ME.

An intriguing observation is that the isotopic values oscillate with an amplitude of $\delta^2\text{H} \sim 0.2\%$ and a recurring time of ~ 25 –30 injections (~ 4 h), which is unrelated to the ME. This noise does not

FIGURE 3 The ME was characterized using consecutive injections of $\sim\text{VSMOW2}$ (injections 1–200) and $\sim\text{SLAP2}$ (injections 200–400). After $\sim\text{SLAP2}$, the system was flushed for 30 h with N_2 gas, and $\sim\text{VSMOW2}$ was injected again (injections 400–600). A–C show unmodified data acquired by the coordinator software running on ^{17}O high precision mode. A, The average $\delta^2\text{H}$ value of each injection, in per mil (‰) (black) and $\delta^2\text{H}$ values of injections discarded by the single injection criteria (SD and slope of a single injection) from panels B and C (red). B, SD of single injections. ME-free points have an $\text{SD} \leq 1$ (black), and samples with have an $\text{SD} > 1$ (red). C, Intra-injection slope of single injections. ME-free points have an absolute slope <0.005 (black), and samples with ME have a slope >0.005 (red). D, Inter-injection slope of the proceeding 15 injections acquired by linear regression. Samples that pass the criteria from panels B and C (black) and those that do not (red). Stabilized ME-free measurements exhibit a slope of less than ± 0.008 (dashed black line). The key points that can be deduced from each set of 200 injections are that reducing instrumental noise does not change the ME, ME lingers for well over 100 injections, and flushing the system with dry N_2 does not remove the ME. ME, memory effect. [Color figure can be viewed at wileyonlinelibrary.com]



seem to be random; however, its source is unclear. As the variations are smaller than the prescribed instrumental uncertainty, we do not evaluate it further.

3.2 | Quantifying the magnitude of ME

In this section, we characterize and quantify the ME between samples that have considerably different isotopic compositions (e.g., VSMOW2 and SLAP2) using the deviation from ME-free samples characterized in the previous section. We tested the effect an enriched sample has on a depleted sample over 200 repeated injections (Figure 3). When injecting a depleted sample ($\delta^2\text{H} = \sim -450\text{‰}$) after an enriched sample ($\delta^2\text{H} = \sim 0\text{‰}$), the enriched sample exerts a large ME on the depleted sample. This enables quantifying the total ME and does not differentiate between potential ME sources in the system (e.g., vaporizer, analyzer cavity, or syringe). Using the Slope15 index (defined earlier), we evaluated the persistence of the ME. Slope15 enters the ± 0.008 range after 89 injections and crosses 0 (i.e., no slope) only after 182 injections (~ 27 h) (Figure 3D). $\delta^2\text{H}$ values of the 45th injection, which, according to Vallet-Coulomb et al.,¹³ should be ME free, are still more than 1‰ higher than those of the ~ 200 th injection. In addition, discarding injections that fail the intra-injection criteria does not assist in hastening the removal of the ME.

The results of the second part of the experiment, where we flushed the instrument with dry N_2 between a depleted and an enriched sample, show a similar ME pattern to that of the first part of the experiment (Slope15 enters the ± 0.008 range after 77 injections and crosses 0 after 140 injections), indicating that flushing the

instrument with dry N_2 does not assist in removing the ME. The results of both parts of the experiment demonstrate that when constructing the VSMOW–SLAP calibration curve, the ME is extremely persistent and, if not considered, will cause a systematic bias to all samples and lab standards evaluated using this calibration curve.

3.3 | Feasibility test

3.3.1 | Characterizing the kick method for a set of bracketing standards and optimizing the number of injections

The previous section showed that the persistence of the ME can cause a substantial bias when constructing a calibration curve. In this section, we examine whether the kick method can shorten the stabilization time required for a given set of bracketing standards. The first set of experiments was conducted using two bracketing standards ($\sim 0\text{‰}$ and $\sim -160\text{‰}$ VSMOW), where the number of kick injections varied in each experiment (0, 3, 5, and 7; Table 2 and Figure 4). We evaluate the results of each experiment using the number of injections required for Slope15 $\leq \pm 0.008\text{‰}$ (i.e., how long it takes the instrument to remove the ME). The results show that for the experiment without a kick, Slope15 enters the ± 0.008 range after 44 injections and crosses 0 only after 80 injections (12 h of repeated injections) (Table 2). When three kick injections are used, an overshoot is observed; that is, the direction of Slope15 changes after 24 injections, reaching a minimum value of -0.018 before returning to acceptable values after 51 injections, indicating the ME of the relatively enriched sample prevailed. We interpret this type of overshoot behavior as an

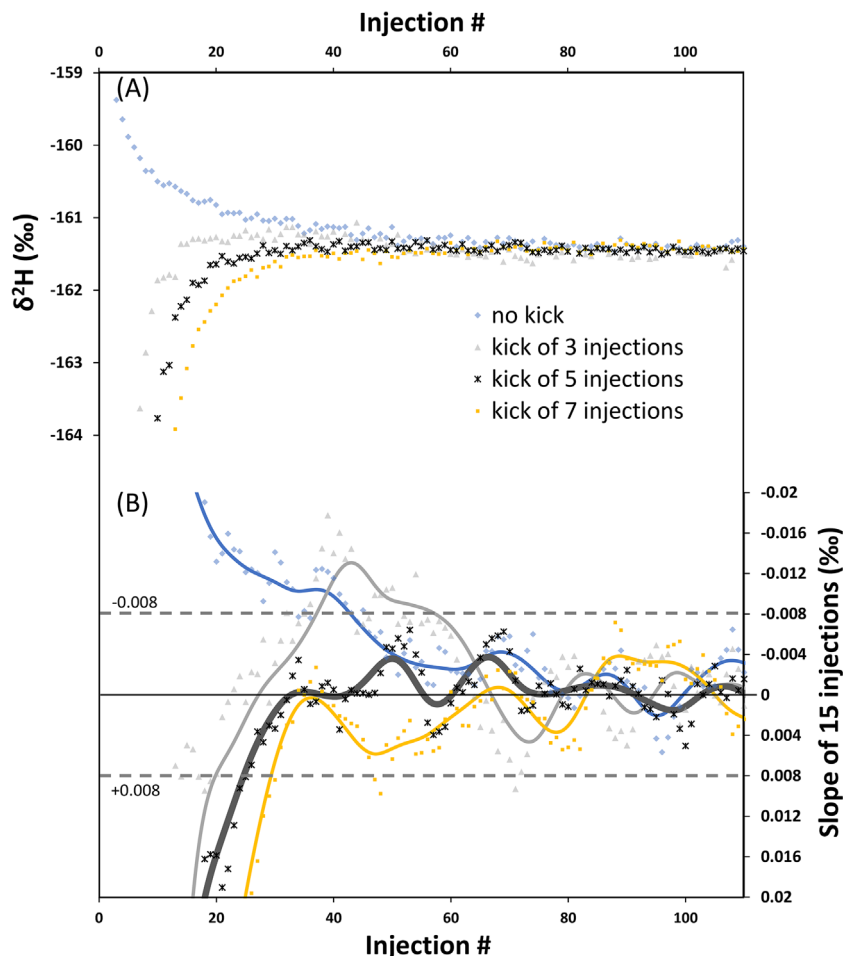
TABLE 2 Experiments testing the number of injections required to remove the ME under various conditions.

Test	Enriched $\delta^2\text{H}$ (‰ VSMOW)	Depleted $\delta^2\text{H}$ (‰ VSMOW)	Difference of $\delta^2\text{H}$ (‰ VSMOW)	Number of kick injections	Number of injections to $ \text{Slope15} \leq 0.008$
1	4	-100	~ 104	0	49
2	4	-100	~ 104	2	39
3	4	-100	~ 104	3	21
4	4	-100	~ 104	5	33
5	4	-160	~ 164	0	44
6	4	-160	~ 164	3	51
7	4	-160	~ 164	5	27
8	4	-160	~ 164	7	31
9	4	-258	~ 262	8	28
10	4	-450	~ 450	0	>100
11	0	-427.5	-427.5	13	60

Note: The test begins by injecting 200 injections of an enriched sample (either 4‰ or 0‰), after which a varying number of kick injections are introduced (with a composition of $\delta^2\text{H} \sim -1000\text{‰}$ and $\delta^{18}\text{O} \sim -220\text{‰}$). The experiment examines how many injections of the depleted sample (of five different compositions) are required to remove the ME to a level of $|\text{Slope15}| \leq 0.008$, that is, what kick is required to remove the ME most efficiently. The different groups of experiments are in different shadings, and the most efficient kick of each group of experiments is in bold.

Abbreviation: ME, memory effect.

FIGURE 4 Testing the kick method. The test begins after 200 injections of an enriched sample ($\sim 0\%$) and compares varying numbers of kick injections (0, 3, 5, 7) of extremely isotopically depleted water ($\delta^2\text{H} \sim -1000\%$), before 200 injections of a depleted sample ($\sim -160\%$). Each experiment is designated a different color (see legend). A, Raw $\delta^2\text{H}$ measurements for each experiment; B, Slope15 for each experiment, where $\text{Slope15} \leq 0.008$ is the cutoff, under which we define the sample ME free. The line through the points is a Gaussian smooth using a 15-injection window. When three kick injections are used, an overshoot is observed, indicating the ME of the relatively enriched sample prevailed. For five kick injections, stabilization of the Slope15 is achieved after 27 injections, after which the slope begins to oscillate around ± 0 . For seven kick injections, the Slope15 stabilizes after 31 injections. The results show that five kick injections effectively flush out the ME in roughly half the number of injections it takes for the no kick to flush out the ME. ME, memory effect. [Color figure can be viewed at wileyonlinelibrary.com]



insufficient kick. Five kick injections achieve stabilization of the Slope15 after 27 injections, after which Slope15 oscillates around ± 0 . For seven kick injections, the Slope15 stabilizes after 31 injections. These results show that the kick method effectively flushes out the ME in roughly half the time it takes for an experiment without a kick (27 vs. 44 injections, respectively). In addition, it is clear that there is an optimal number of injections for a set of bracketing standards for which the reduction of the ME is the fastest and most persistent (in the case of 0% to -160% , the ideal number is five injections). It is also worth noting that even a sub-optimal kick (i.e., too many or too few injections) is better than no kick at all.

3.3.2 | Quantifying the number of injections for varying bracketing standards

To test whether the number of kick injections is a function of the difference between the bracketing standards, we conducted a similar experiment to that presented in Section 3.3.1, this time with a smaller difference between the bracketing standards (0% to -100%), and ran four experiments using different amounts of kick injections (0, 2,

3, and 5; Figure 5). The results show that for the run with no kick, Slope15 does not reach permanent positive values until the 56th injection. A kick of two injections shows a very small overshoot: after 15 injections, the Slope15 enters the ± 0.008 range; however, the Slope15 changes direction to negative values reaching -0.008 at the 39th injection. The optimal kick is identified as three injections, where Slope15 enters the ± 0.008 range after 21 injections and oscillates around ± 0 . A kick of five injections causes the Slope15 index to enter the ± 0.008 range after a longer time of 33 injections. These results, combined with the previous set of experiments (Section 3.3.1), indicate that the optimal number of kick injections for minimizing stabilization time varies as a function of the difference between the bracketing standards and that the optimal number of injections is three injections per 100% difference. In addition, there are characteristic behaviors of overshooting and undershooting of the number of kicks, as seen in both sets of experiments.

Following these results, we validated the required kick for minimal stabilization time using two sets of IAEA-certified standards: (a) VSMOW2 followed by GRESP (a 258% difference), which required 8 kick injections (Figure S1 [supporting information]); and (b) VSMOW2 followed by SLAP2 (a 427.5% difference), which

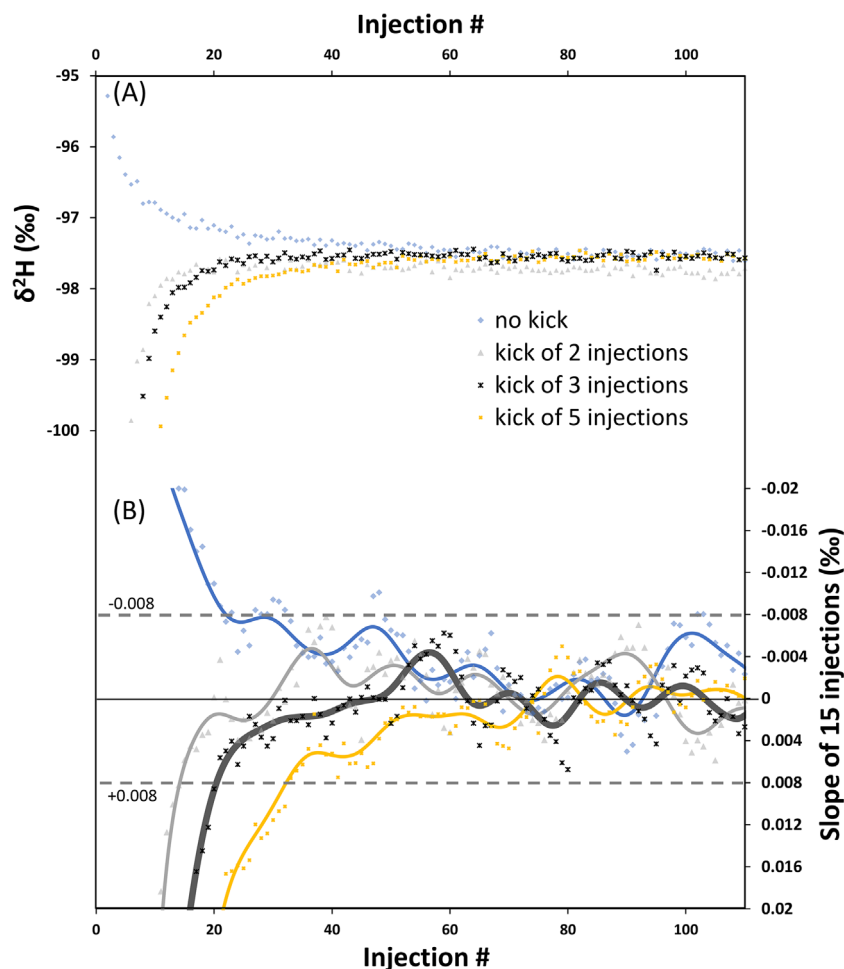


FIGURE 5 Testing the kick method for a smaller difference between standards (0‰ and -100‰), and varying numbers of kick injections (0, 2, 3, 5). The optimal kick number for a 100‰ difference between standards is three injections. For the run with no kick, Slope15 does not reach permanent positive values until the 56th injection. A kick of two injections shows a very small overshoot. The optimal kick is identified as three injections, where Slope15 values enter the ± 0.008 range after 21 injections and oscillates around ± 0 . A kick of five injections causes the Slope15 index to enter the 0.008 range after a longer time of 33 injections. The experiments with two and five kick injections show the same characteristic undershoot and overshoot, respectively, as that seen in Figure 4. [Color figure can be viewed at wileyonlinelibrary.com]

required 13 kick injections. The characteristic pattern of rapid and smooth reduction of the ME in both experiments indicates that 8 and 13 injections, respectively, are the correct number of required injections to achieve minimal stabilization time. These results strengthen the results of the first two sets of experiments, showing that the amount of kick injections achieving the minimal stabilization time is proportional to the difference between the enriched and depleted samples.

In all cases presented, the structure of the ME decline is similar, and the stabilization time is shorter by roughly half the number of injections than that of experiments without a kick. This is most substantial for the VSMOW-SLAP calibration because it reduces the number of injections required to reach an ME-free measurement by ~ 60 injections (~ 9 h).

3.4 | Validation 1: Testing the kick method for known international standards

In the previous section, we showed that the kick method produces faster stabilization times and ME removal; however, the precision of

the measurements and reproducibility were not evaluated. To test the precision and accuracy of the kick method, we implemented it when constructing the VSMOW-SLAP calibration curve and measured certified secondary international standards (USGS45, 47, 49, 50 and GRESP) as well as one interlab standard,^{24,33-37} which were treated as unknowns (Figure 6, Table 4, and detailed sequence in Table 3). When constructing the calibration curve of the primary standards (VSMOW2 and SLAP2), the Slope15 index was confirmed to be below 0.008. The results show that GRESP and the four USGS standards are within the certified values with lower SD than recently published papers, indicating better reproducibility between independent sessions (Table 3). Comparisons of ^{17}O -excess values with recently published literature^{7,8,13,14,37,38} show that our method achieves remarkably small SDs and high reproducibility.

3.5 | Validation 2: Testing the kick method during routine measurements

In this section, we discuss the usage of the kick method in routine measurements to verify that there is no bias due to ME and to

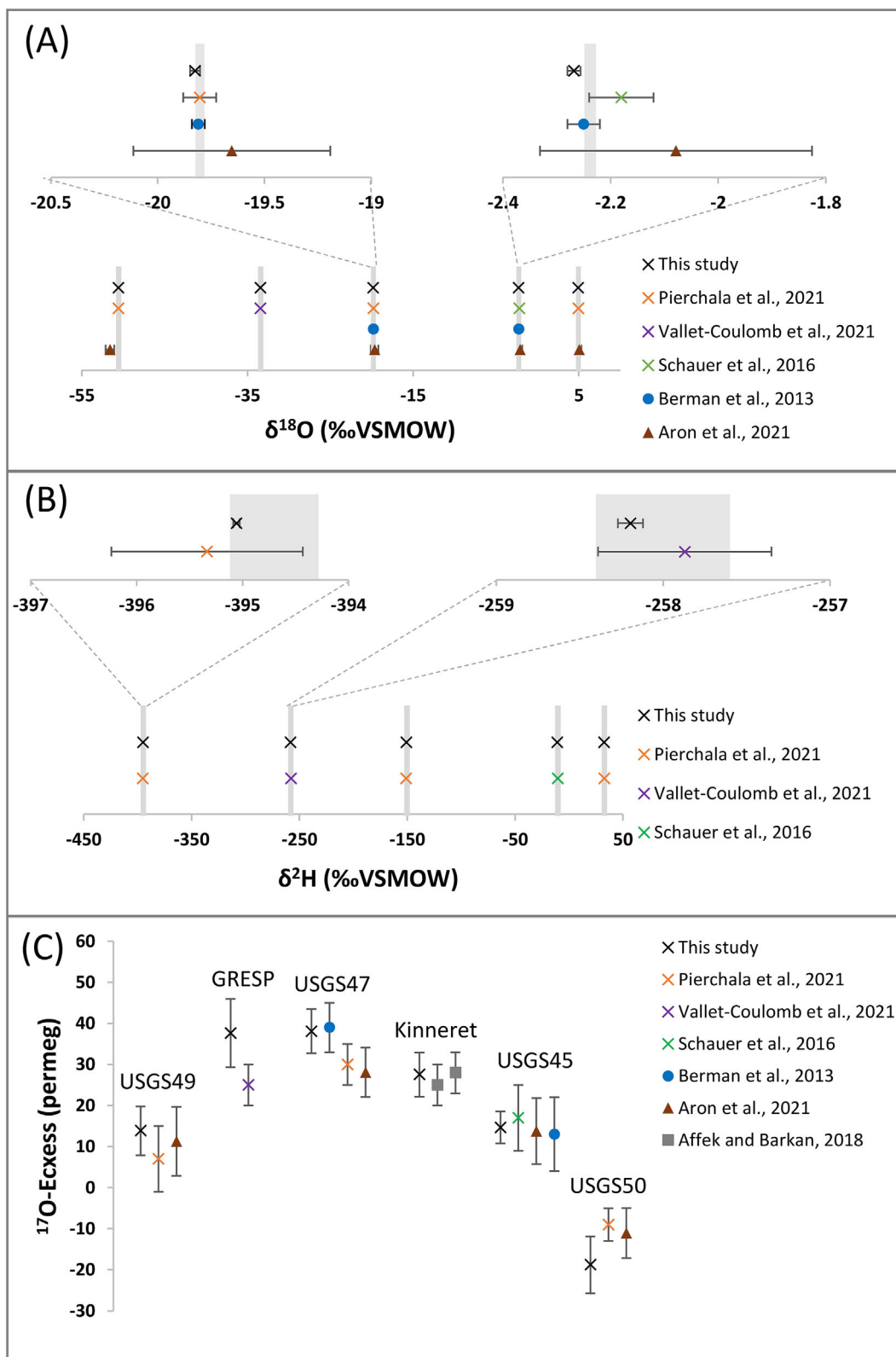


FIGURE 6 Analytical precision and accuracy of five international lab standards measured using the kick method compared with other recently published methodologies. Certified uncertainties are presented as gray bars. Error bars represent the intersession SD. A, $\delta^{18}\text{O}$ with representative enlargements. “X” icons are measurements done using the same instrument. B, Same as A for $\delta^2\text{H}$; note that the measured uncertainty is nearly an order of magnitude lower than the certified and published uncertainty. C, ^{17}O -excess values for the international standards as well as one interlab standard (Kinneret) in the order of isotopic composition from depleted to enriched. The interlab standard was measured by two different IRMS methods after Affek and Barkan.³⁷ Values agree with recent literature with similar or better reproducibility. See Table 3 for further details. IRMS, isotope ratio mass spectrometer. [Color figure can be viewed at wileyonlinelibrary.com]

TABLE 3 Comparisons of measured isotopic values using our method with recently published literature.

	$\delta^{18}\text{O}$		$\delta^2\text{H}$		^{17}O -excess	
	‰	SD	‰	SD	permeg	SD
USGS49	-50.55 ± 0.04		-394.7 ± 0.4		...	
This study	-50.570	0.027	-395.07	0.01	14	6
Pierchala et al. (2021)	-50.588	0.033	-395.34	0.90	7	8
Aron et al. (2021) ^a	-51.595	0.523	11	8
GRESF	-33.4 ± 0.04		-258 ± 0.4		...	
This study	-33.426	0.028	-258.20	0.08	38	8
Vallet-Coulomb et al. (2021)	-33.45	0.034	-257.87	0.52	25	5
USGS47	-19.8 ± 0.04		-150.2 ± 0.5		...	
This study	-19.825	0.020	-150.94	0.04	38	5
Berman et al. (2013)	-19.81	0.03	39	6
Pierchala et al. (2021)	-19.803	0.077	-151.2	0.4	30	5
Aron et al. (2021) ^a	-19.653	0.461	28	6
USGS45	-2.238 ± 0.011		-10.3 ± 0.4		...	
This study	-2.268	0.012	-10.82	0.03	15	4
Schauer et al. (2016)	-2.180	0.06	-10.48	0.39	17	8
Aron et al. (2021) ^a	-2.078	0.253	14	8
Berman et al. (2013)	-2.25	0.03	13	9
USGS50	4.95 ± 0.02		32.8 ± 0.4		...	
This study	4.918	0.013	32.37	0.05	-19	7
Pierchala et al. (2021)	4.964	0.035	32.8	0.33	-9	4
Aron et al. (2021) ^a	5.066	0.226	-11	6
Kinneret						
This study	-5.265	0.013	-23.98	0.04	28	5
Affek and Barkan (2018)	25	5
Affek and Barkan (2018)	28	5

Note: Certified values and their corresponding uncertainties are as published by IAEA and USGS^{28–36} (bold). Uncertainty of the measured values is the SD from the published literature.^{7,8,13,14,37,38} The interlab standard (Kinneret) is presented by two different IRMS methods after Affek and Barkan.³⁷ Abbreviations: IAEA, International Atomic Energy Agency; IRMS, isotope ratio mass spectrometer; USGS, United States Geological Survey.

^aAverage and SD calculated from the supplementary material of Aron et al.³⁸

quantify the measurement uncertainty. To evaluate the precision and accuracy of samples during routine measurements, we examine the difference between expected and measured isotopic values of quality assurance standards, which were dispersed among unknown samples in three separate runs. Evaluating the quality assurance standards provides a direct quantification of precision and accuracy and does not require error propagation formulas (e.g., Pierchala et al.¹⁵), which have been shown to provide overly optimistic values.^{4,26} For each run, we present three statistical analyses (Table 4). To verify the bias, we examine the average difference between the measured and known values and the SD of this difference (1σ). In all cases, the average differences from the known values are smaller than 1σ . This effectively indicates that our method does not produce a systematic bias (i.e., quality assurance

standards are not consistently biased toward positive or negative values). To estimate the uncertainty of a run, we use the average of the absolute differences between the measured and known values and report these values as our measurement uncertainty. The average uncertainty of the absolute differences of the three runs is 0.03‰, 0.2‰, and 5 permeg for $\delta^{18}\text{O}$, $\delta^2\text{H}$, and ^{17}O -excess of the known values, respectively (Table 4). An important observation from Table 4 is that when measurements are noisy (higher intra-injection slope and SD), the overall uncertainty of the quality assurance standards rises, but an instrumental bias is not observed, indicating that the intra-injection noise is scattered randomly and does not produce a bias in a specific direction. We conclude that when implemented in routine measurements, the kick method improves overall accuracy.

TABLE 4 Quantifying uncertainty and bias of three validation runs.

		$\delta^{17}\text{O}$ miss (‰)	$\delta^{18}\text{O}$ miss (‰)	$\delta^2\text{H}$ miss (‰)	^{17}O -excess miss (permeg)
Run #1 (n = 9)	Average	0.004	0.014	0.19	−4
	SD	0.021	0.040	0.34	8
	Absolute average	0.016	0.033	0.24	6
Run #2 (n = 12)	Average	0.012	0.020	0.07	1
	SD	0.015	0.031	0.27	6
	Absolute average	0.015	0.031	0.20	4
Run #3 (n = 9)	Average	0.023	0.043	0.20	0
	SD	0.019	0.033	0.30	7
	Absolute average	0.025	0.043	0.27	6
Average	Average	0.013	0.025	0.15	0
	SD	0.019	0.035	0.30	7
	Absolute average	0.018	0.035	0.23	5

Note: In each run, three quality assurance standards with known isotopic values were interspersed between unknown samples and those treated as unknowns. Uncertainty and bias are quantified as the average difference between measured and expected values, SD, and the average of the absolute values of the difference between measured and expected values. In all cases, the average is smaller than the SD, indicating that within analytical uncertainty, there is no bias. In bold, the combined average, SD and absolute average of all quality assurance measurements from the three runs.

4 | CONCLUSIONS

Cavity ring-down spectroscopy is greatly affected by the ME, a sample-to-sample carryover. This study demonstrates the persistence of the ME, which is often overlooked in the routine analysis of natural water samples, and particularly affects the VSMOW–SLAP calibration curve and can create a systematic bias of all measurements. We first defined a set of statistical criteria to identify the ME and showed that it persists for a very long time in the instrument. We then presented a simple, time-efficient, and readily available method that entails the introduction of a few kick injections of extreme isotopic water into the system, which counterbalances the ME. We showed that the number of kick injections required to remove the ME is proportional to the difference between the bracketing samples or standards (three injections of ~1000‰ water for each 100‰ difference of $\delta^2\text{H}$ values between samples). The results show that using our kick method substantially lowers the stabilization time for creating an ME-free measurement and is particularly time saving when constructing the VSMOW–SLAP calibration curve. We verified our method using six certified international and interlab standards that span a wide range of isotopic compositions and derived a generalized protocol for application. Implementing our suggested method in routine measurements removes bias, and we achieved typical uncertainty values of 0.03‰, 0.2‰, and 5 permeg for $\delta^{18}\text{O}$, $\delta^2\text{H}$ and, ^{17}O -excess values, respectively.

AUTHOR CONTRIBUTIONS

Jonathan Keinan: Conceptualization; data curation; formal analysis; investigation; methodology; software; validation; visualization; writing—original draft. **Yonaton Goldsmith:** Conceptualization; funding acquisition; investigation; methodology; supervision; writing—review and editing.

ACKNOWLEDGMENTS

The authors thank Eugeni Barkan, Hagit Affek, and Boaz Luz for fruitful discussions and for sharing reference waters and Nadav Lensky for overall assistance with this research. The authors also thank Lilach Gonen and Ofer Cohen for assisting in lab work and the two anonymous reviewers for their insightful comments. This work was supported by the Israel Science Foundation (no. 2229/21) and by the Climate Crisis Scholarship of the Jewish National Fund awarded to J.K.

PEER REVIEW

The peer review history for this article is available at <https://www.webofscience.com/api/gateway/wos/peer-review/10.1002/rcm.9600>.

DATA AVAILABILITY STATEMENT

Data are available in article supplementary material.

ORCID

Jonathan Keinan  <https://orcid.org/0000-0001-5185-9753>

Yonaton Goldsmith  <https://orcid.org/0000-0003-0398-9005>

REFERENCES

1. Wassenaar LI, Ahmad M, Aggarwal P, et al. Worldwide proficiency test for routine analysis of $\delta^2\text{H}$ and $\delta^{18}\text{O}$ in water by isotope-ratio mass spectrometry and laser absorption spectroscopy. *Rapid Commun Mass Spectrom*. 2012;26(15):1641–1648. doi:10.1002/rcm.6270
2. Wassenaar LI, Coplen TB, Aggarwal PK. Approaches for achieving long-term accuracy and precision of $\delta^{18}\text{O}$ and $\delta^2\text{H}$ for waters analyzed using laser absorption spectrometers. *Environ Sci Technol*. 2014;48(2):1123–1131. doi:10.1021/es403354n
3. Wassenaar LI, Terzer-Wassmuth S, Douence C, Araguas-Araguas L, Aggarwal PK, Coplen TB. Seeking excellence: an evaluation of 235 international laboratories conducting water isotope analyses by

- isotope-ratio and laser-absorption spectrometry. *Rapid Commun Mass Spectrom.* 2018;32(5):393-406. doi:[10.1002/rcm.8052](https://doi.org/10.1002/rcm.8052)
4. Wassenaar L, Terzer-Wassmuth S, Douence C. Progress and challenges in dual- and triple-isotope ($\delta^{18}\text{O}$, $\delta^2\text{H}$, $\Delta^{17}\text{O}$) analyses of environmental waters: an international assessment of laboratory performance. *Rapid Commun Mass Spectrom.* 2021;35(24):1-12. doi:[10.1002/rcm.9193](https://doi.org/10.1002/rcm.9193)
 5. Ahmad M, Aggarwal P, van Duren M, et al. *Final Report on Fourth Interlaboratory Comparison Exercise for $\delta^2\text{H}$ and $\delta^{18}\text{O}$ Analysis of Water Samples (WICO2011)*. Int Atomic Energy Agency; 2012.
 6. Steig EJ, Gkinis V, Schauer AJ, et al. Calibrated high-precision ^{17}O -excess measurements using cavity ring-down spectroscopy with laser-current-tuned cavity resonance. *Atmos Meas Tech.* 2014;7(8):2421-2435. doi:[10.5194/amt-7-2421-2014](https://doi.org/10.5194/amt-7-2421-2014)
 7. Berman ESF, Levin NE, Landais A, Li S, Owano T. Measurement of $\delta^{18}\text{O}$, $\delta^{17}\text{O}$, and ^{17}O -excess in water by off-axis integrated cavity output spectroscopy and isotope ratio mass spectrometry. *Anal Chem.* 2013;85(21):10392-10398. doi:[10.1021/ac402366t](https://doi.org/10.1021/ac402366t)
 8. Schauer AJ, Schoenemann SW, Steig EJ. Routine high-precision analysis of triple water-isotope ratios using cavity ring-down spectroscopy. *Rapid Commun Mass Spectrom.* 2016;30(18):2059-2069. doi:[10.1002/rcm.7682](https://doi.org/10.1002/rcm.7682)
 9. Lis G, Wassenaar LI, Hendry MJ. High-precision laser spectroscopy D/H and $^{18}\text{O}/^{16}\text{O}$ measurements of microliter natural water samples. *Anal Chem.* 2008;80(1):287-293. doi:[10.1021/ac701716q](https://doi.org/10.1021/ac701716q)
 10. van Geldern R, Barth JAC. Optimization of instrument setup and post-run corrections for oxygen and hydrogen stable isotope measurements of water by isotope ratio infrared spectroscopy (IRIS). *Limnol Oceanogr Methods.* 2012;10(12):1024-1036. doi:[10.4319/lom.2012.10.1024](https://doi.org/10.4319/lom.2012.10.1024)
 11. Gröning M. Improved water $\delta^2\text{H}$ and $\delta^{18}\text{O}$ calibration and calculation of measurement uncertainty using a simple software tool. *Rapid Commun Mass Spectrom.* 2011;25(19):2711-2720. doi:[10.1002/rcm.5074](https://doi.org/10.1002/rcm.5074)
 12. de Graaf S, Vonhof HB, Levy EJ, Markowska M, Haug GH. Isotope ratio infrared spectroscopy analysis of water samples without memory effects. *Rapid Commun Mass Spectrom.* 2021;35(8):1-12. doi:[10.1002/rcm.9055](https://doi.org/10.1002/rcm.9055)
 13. Vallet-Coulomb C, Couapel M, Sonzogni C. Improving memory effect correction to achieve high-precision analysis of $\delta^{17}\text{O}$, $\delta^{18}\text{O}$, $\delta^2\text{H}$, ^{17}O -excess and d-excess in water using cavity ring-down laser spectroscopy. *Rapid Commun Mass Spectrom.* 2021;35(14):e9108. doi:[10.1002/rcm.9108](https://doi.org/10.1002/rcm.9108)
 14. Pierchala A, Rozanski K, Dulinski M, Gorczyca Z, Czub R. Triple-isotope calibration of in-house water standards supplemented by determination of ^{17}O content of USGS49-50 reference materials using cavity ring-down laser spectrometry. *Isotopes Environ Health Stud.* 2021;57(3):254-261. doi:[10.1080/10256016.2021.1875222](https://doi.org/10.1080/10256016.2021.1875222)
 15. Pierchala A, Rozanski K, Dulinski M, Gorczyca Z, Marzec M, Czub R. High-precision measurements of $\delta^2\text{H}$, $\delta^{18}\text{O}$ and $\delta^{17}\text{O}$ in water with the aid of cavity ring-down laser spectroscopy. *Isotopes Environ Health Stud.* 2019;55(3):290-307. doi:[10.1080/10256016.2019.1609959](https://doi.org/10.1080/10256016.2019.1609959)
 16. Thiel PA, Madey TE. The interaction of water with solid surfaces: fundamental aspects. *Surf Sci Rep.* 1987;7(6-8):211-385. doi:[10.1016/0167-5729\(87\)90001-X](https://doi.org/10.1016/0167-5729(87)90001-X)
 17. Dobrozemsky R, Menhart S, Buchtela K. Residence times of water molecules on stainless steel and aluminum surfaces in vacuum and atmosphere. *J Vac Sci Technol A.* 2007;25(3):551-556. doi:[10.1116/1.2718958](https://doi.org/10.1116/1.2718958)
 18. Morrison J, Brockwell T, Merren T, Fourel F, Phillips AM. On-line high-precision stable hydrogen isotopic analyses on nanoliter water samples. *Anal Chem.* 2001;73(15):3570-3575. doi:[10.1021/ac001447t](https://doi.org/10.1021/ac001447t)
 19. Outrequin C, Alexandre A, Vallet-Coulomb C, et al. The triple oxygen isotope composition of phytoliths, a new proxy of atmospheric relative humidity: controls of soil water isotope composition, temperature, CO_2 concentration and relative humidity. *Clim Past.* 2021;17(5):1881-1902. doi:[10.5194/cp-17-1881-2021](https://doi.org/10.5194/cp-17-1881-2021)
 20. Kim S, Han C, Moon J, Han Y, Do HS, Lee J. An optimal strategy for determining triple oxygen isotope ratios in natural water using a commercial cavity ring-down spectrometer. *Geosc J.* 2022;26(5):637-647. doi:[10.1007/s12303-022-0009-y](https://doi.org/10.1007/s12303-022-0009-y)
 21. Guidotti S, Jansen HG, Aerts-Bijma AT, Verstappen-Dumoulin BMAA, van Dijk G, Meijer HAJ. Doubly Labelled Water analysis: preparation, memory correction, calibration and quality assurance for $\delta^2\text{H}$ and $\delta^{18}\text{O}$ measurements over four orders of magnitudes. *Rapid Commun Mass Spectrom.* 2013;27(9):1055-1066. doi:[10.1002/rcm.6540](https://doi.org/10.1002/rcm.6540)
 22. Hachgenei N, Vaury V, Nord G, Spadini L, Duwig C. Faster and more precise isotopic water analysis of discrete samples by predicting the repetitions' asymptote instead of averaging last values. *MethodsX.* 2022;9:101656. doi:[10.1016/j.mex.2022.101656](https://doi.org/10.1016/j.mex.2022.101656)
 23. de Graaf S, Vonhof HB, Weissbach T, et al. A comparison of isotope ratio mass spectrometry and cavity ring-down spectroscopy techniques for isotope analysis of fluid inclusion water. *Rapid Commun Mass Spectrom.* 2020;34(16):e8837. doi:[10.1002/rcm.8837](https://doi.org/10.1002/rcm.8837)
 24. Qu D, Tian L, Zhao H, Yao P, Xu B, Cui J. Demonstration of a memory calibration method in water isotope measurement by laser spectroscopy. *Rapid Commun Mass Spectrom.* 2020;34(8):e8689. doi:[10.1002/rcm.8689](https://doi.org/10.1002/rcm.8689)
 25. Schoenemann SW, Schauer AJ, Steig EJ. Measurement of SLAP2 and GISP $\delta^{17}\text{O}$ and proposed VSMOW-SLAP normalization for $\delta^{17}\text{O}$ and $^{17}\text{O}_{\text{excess}}$. *Rapid Commun Mass Spectrom.* 2013;27(5):582-590. doi:[10.1002/rcm.6486](https://doi.org/10.1002/rcm.6486)
 26. Gröning M. Some pitfalls in the uncertainty evaluation of isotope delta reference materials. *Accredit Qual Assur.* 2023;28:101-114. doi:[10.1007/S00769-022-01527-6/TABLES/4](https://doi.org/10.1007/S00769-022-01527-6/TABLES/4)
 27. York D, Evensen NM, Martínez ML, De Basabe Delgado J. Unified equations for the slope, intercept, and standard errors of the best straight line. *Am J Physiol.* 2004;72(3):367-375. doi:[10.1119/1.1632486](https://doi.org/10.1119/1.1632486)
 28. Lorenz JM, Qi H, Coplen TB. Antarctic ice-core water (USGS49)—a new isotopic reference material for $\delta^2\text{H}$ and $\delta^{18}\text{O}$ measurements of water. *Geostand Geoanal Res.* 2017;41(1):63-68. doi:[10.1111/GGR.12135](https://doi.org/10.1111/GGR.12135)
 29. Lorenz JM, Tarbox L, Buck B, Qi H, Coplen TB. Biscayne aquifer drinking water (USGS45): a new isotopic reference material for $\delta^2\text{H}$ and $\delta^{18}\text{O}$ measurements of water. *Rapid Commun Mass Spectrom.* 2014;28(19):2031-2034. doi:[10.1002/rcm.6988](https://doi.org/10.1002/rcm.6988)
 30. Qi H, Lorenz JM, Coplen TB, Tarbox L, Mayer B, Taylor S. Lake Louise Water (USGS47): a new isotopic reference water for stable hydrogen and oxygen isotope measurements. *Rapid Commun Mass Spectrom.* 2014;28(4):351-354. doi:[10.1002/rcm.6789](https://doi.org/10.1002/rcm.6789)
 31. Coplen TB, Wassenaar LI, Mukwaya C, Qi H, Lorenz JM. A new isotopic reference material for stable hydrogen and oxygen isotope-ratio measurements of water—USGS50 Lake Kyoga Water. *Rapid Commun Mass Spectrom.* 2015;29(21):2078-2082. doi:[10.1002/rcm.7369](https://doi.org/10.1002/rcm.7369)
 32. International Atomic Energy Agency. Reference Sheet for Certified Reference Material: GRESP, Greenland Summit Precipitation water. Accessed April 3, 2023.
 33. U.S. Geological Survey. RSIL: Report of Stable Isotopic Composition for reference material USGS50. Accessed April 3, 2023. <https://www.usgs.gov/media/files/rsil-report-stable-isotopic-composition-reference-material-usgs50>
 34. U.S. Geological Survey. RSIL: Report of Stable Isotopic Composition for reference material USGS49. Accessed April 3, 2023. <https://www.usgs.gov/media/files/rsil-report-stable-isotopic-composition-reference-material-usgs49>

35. U.S. Geological Survey. RSIL: Report of Stable Isotopic Composition for reference material USGS47. Accessed April 3, 2023. <https://www.usgs.gov/media/files/rsil-report-stable-isotopic-composition-reference-material-usgs47>
36. U.S. Geological Survey. RSIL: Report of Stable Isotopic Composition for reference material USGS45. Accessed April 3, 2023. <https://www.usgs.gov/media/files/rsil-report-stable-isotopic-composition-reference-material-usgs45>
37. Affek HP, Barkan E. A new method for high-precision measurements of $^{17}\text{O}/^{16}\text{O}$ ratios in H_2O . *Rapid Commun Mass Spectrom*. 2018; 32(23):2096-2097. doi:10.1002/rcm.8290
38. Aron PG, Levin NE, Beverly EJ, et al. Triple oxygen isotopes in the water cycle. *Chem Geol*. 2021;565(October 2020):120026. doi:10.1016/j.chemgeo.2020.120026
39. Spangenberg JE. Caution on the storage of waters and aqueous solutions in plastic containers for hydrogen and oxygen stable isotope analysis. *Rapid Commun Mass Spectrom*. 2012;26(22):2627-2636. doi:10.1002/rcm.6386

SUPPORTING INFORMATION

Additional supporting information can be found online in the Supporting Information section at the end of this article.

How to cite this article: Keinan J, Goldsmith Y. A simple method for rapid removal of the memory effect in cavity ring-down spectroscopy water isotope measurements. *Rapid Commun Mass Spectrom*. 2023;37(19):e9600. doi:10.1002/rcm.9600